

## Fractal properties of lysozyme: A neutron scattering study

S. G. Lushnikov and A. V. Svanidze

*Ioffe Physical Technical Institute, RAS, 194021, St. Petersburg, Russia*

S. N. Gvasaliya

*Laboratory for Neutron Scattering, ETH Zurich, CH-5232 Villigen, Switzerland and Paul Scherrer Institut, CH-5232 Villigen, Switzerland*

G. Torok and L. Rosta

*Budapest Neutron Centre, Konkoly Thege 29-33, Budapest H-1525, Hungary*

I. L. Sashin

*Frank Laboratory for Neutron Physics, JINR, 141980 Dubna, Russia*

(Received 24 August 2008; published 24 March 2009)

The spatial structure and dynamics of hen egg white lysozyme have been investigated by small-angle and inelastic neutron scattering. Analysis of the results was carried using the fractal approach, which allowed determination of the fractal and fracton dimensions of lysozyme, i.e., consideration of the protein structure and dynamics by using a unified approach. Small-angle neutron scattering studies of thermal denaturation of lysozyme have revealed changes in the fractal dimension in the vicinity of the thermal denaturation temperature that reflect changes in the spatial organization of protein.

DOI: [10.1103/PhysRevE.79.031913](https://doi.org/10.1103/PhysRevE.79.031913)

PACS number(s): 87.14.E-, 87.15.A-, 87.15.H-, 87.64.Bx

The mechanism of protein functioning is of vital importance for understanding of the activity of living organisms at the molecular level. At present research efforts of many teams all over the world are focused on the investigations of proteins, however, few attempts have been made to treat the protein structure and dynamics in the framework of a unified approach. In this paper we demonstrate the use of the fractal approach for description of protein properties from a single point of view. The fractal geometry is a suitable tool for analysis of the spatial organization and dynamics of disordered or partly ordered media [1,2], and it is not surprising that from the moment of development of the fractal theory by Mandelbrot there have been numerous efforts to describe the protein topology by using the fractal approach. For the first time this approach to the protein structure description was reported in [3] where the fractal dimensions of some hemoproteins and ferredoxin were found from the temperature dependences of the spin-lattice relaxation time of  $\text{Fe}^{3+}$ . In the calculations of the fractal dimension  $D_f$  the protein molecule was regarded as a homogeneous isotropic body with mass  $M$  consisting of a polypeptide chain of length  $L$ . It was shown that  $D_f$  is, on the average,  $1.65 \pm 0.04$  for several hemoproteins [3].

Later another fractal model of a protein molecule [4] was suggested. In this model the backbone of a protein molecule in the form of a folded massless linear chain is considered for simplicity, and side groups are ignored. This chain forms a self-avoiding linear fractal, its separate parts being connected by virtual massless springs. In a more recent model the protein molecule is considered to be a “mass” fractal [5]. Note that in the case of the mass fractal the law of increasing mass of a fractal object is described by the function of its linear sizes  $M(r) \propto r^{D_f}$ ; i.e., the density becomes a decreasing function of the fractal object size  $\rho(r) \propto r^{D_f-D}$ ,  $D > D_f$ , where  $D$  is the topological dimension of the space into which the fractal is embedded [1,2]. By using the mass fractal model

for computer simulation (based on the x-ray structural data obtained from the protein data bank), fractal dimensions of 200 different proteins including from 100 to 1000 amino-acid residues have been determined [5]. It has been shown that the fractal dimension ranges from 2.25 to 2.75, and generally the smaller the protein, the lower its  $D_f$  [5].

It is important to note that changes in the spatial organization of a protein molecule result in changes in its fractal dimension. In particular, when subjected to the action of different denaturants, a native protein molecule can pass into the state of a Gaussian chain. Changes in the fractal dimension at protein transformation have been demonstrated in the experiments on denaturation of bovine serum albumin (BSA) by lithium dodecyl sulfate that binds with each amino-acid residue of the polypeptide chain and forms micellelike structures along the molecule backbone [6]. It has been found that BSA denaturation results in a decrease in its fractal dimension from 2.30 to 1.76. Thus, fractal dimension can be used as a quantitative characteristic that describes the spatial organization of a protein and its changes at phase transformation.

If the fractal approach is used for description of a protein, then, as follows from the Alexander-Orbach conjecture, the low-frequency part of the protein vibration spectrum must contain a localized excitation at a fractal, i.e., a fracton (the properties of this excitation were described in detail in a review [2]), whose dispersion law in a certain frequency range is  $\omega \propto k^{D_f \tilde{d}}$ , where  $\tilde{d}$  is the fracton dimension. The protein vibration spectrum was analyzed theoretically in [7]. ben-Avraham [7] obtained numerical estimates of the fractal and fracton dimensions of g-actin and suggested an explanation of specific features of the low-frequency protein dynamics based on the fractality of the protein structure. Model calculations have shown that fracton dimensions of proteins range from 1.3 to 1.9 (Ref. [8] and references therein). The

function of density of vibrational states of different proteins has been widely studied experimentally [9–11]. For instance, analysis of the low-frequency region of the function of density of vibrational states of superoxide dismutase allowed identification of the Debye regime in the 1–5 meV energy range in the temperature interval of 50–300 K [10]. Later, analysis of the generalized density of states function revealed that both the Debye and fracton regimes were realized in the low-frequency region of the vibration spectrum of lysozyme [12].

The goal of our work is to describe the protein structure and dynamics in the framework of the fractal approach and to demonstrate that this approach is applicable to protein description and allows quantitative estimation of changes in the protein spatial organization at phase transformations (thermal denaturation). The object was hen egg white lysozyme that consists of 129 amino-acid residues and has the globular tertiary structure stabilized by four disulfide bonds. This protein is usually used as a model object for studying protein properties because of its availability and easiness for utilization and relative stability. So it is the most studied protein in comparison with others. For the investigations, small-angle neutron scattering (SANS) and inelastic neutron scattering (INS) techniques were used.

SANS spectra were recorded at scattering wave vectors  $Q=(4\pi/\lambda)\sin \theta/2$  ranging from 0.0401 to 0.5088  $\text{\AA}^{-1}$  by a small-angle neutron «Yellow Submarine» diffractometer (Budapest Neutron Center, Hungary). Measurements were performed for two detector positions, i.e., at distances of 1.3 and 1.5 m from the sample, at the neutron wavelength  $\lambda = 3.38$   $\text{\AA}$ . The neutrons scattered in the sample were detected by a two-dimensional position-sensitive detector 64  $\times$  64  $\text{cm}^2$  in size with resolution of 10  $\times$  10  $\text{mm}^2$ . Solutions of lysozyme (hen egg white lysozyme, Fluka) with concentrations of 50 and 250 mg/ml in sodium acetate buffer (0.1M, pH=4.6) were prepared by using heavy water ( $\text{D}_2\text{O}$ ). Both solutions contained 0.02% sodium azide to prevent bacterial contamination. In the experiment the solutions were heated from 300 to 347.5 K. Prior to spectrum recording, the sample was kept for 10 min at each temperature of measurements. The temperature was maintained with an accuracy of  $\pm 0.3^\circ$ . The signal accumulation time was 10 min. The measurements yielded the dependence of scattering intensity on wave vector  $I(q)$ . When the experimental data were processed, the contributions into scattering made by the instrumental factors [13] and scattering from the pure solvent were subtracted. The data were normalized to the neutron scattering in pure water and also to a corresponding protein concentration in the solution.

INS experiments were performed at a time-of-flight KDSOG-M spectrometer with inverse geometry placed at the IBR-2 pulsed reactor (LNP, JINR, Dubna). The measurements were performed simultaneously for eight scattering angles (30°, 50°, 70°, 90° and 80°, 100°, 120°, 140°) with a final energy of 4.85 meV and a resolution at the elastic position of  $\sim 0.6$  meV. After subtracting the contribution from the sample holder and normalizing by comparison with vanadium standard, the spectra obtained for the scattering angles were treated in the framework of a one-phonon incoherent approximation by using relation

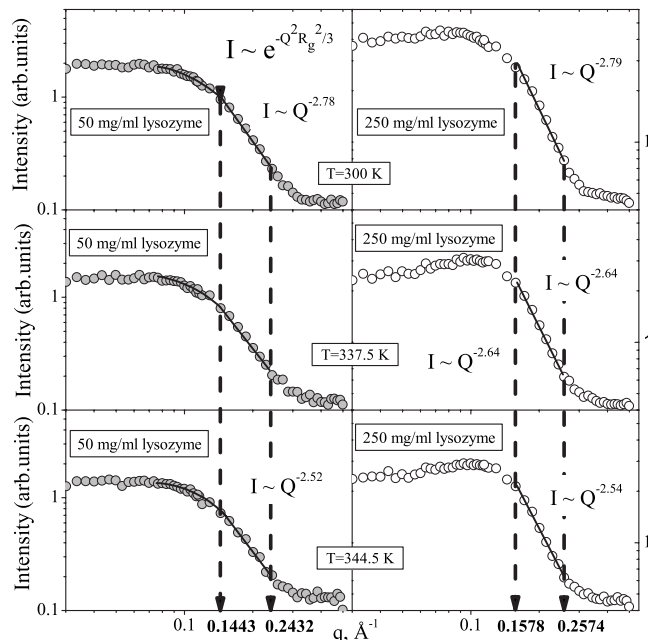


FIG. 1. Small-angle neutron scattering of lysozyme at different temperatures in the log-log scale. The circles show experimental results, the solid line shows the results calculated by using Eqs. (2) and (3). Left panel of the figure represents the results obtained for the solution of lysozyme with concentration of 50 mg/ml while right panel shows the results for the 250 mg/ml concentration in sodium acetate buffer.

$$G(\omega) = \frac{\omega}{n(\omega) + 1} \frac{\vec{k}_0}{k_1} \frac{1}{Q^2} \left( \frac{d^2 \sigma}{d\Omega d\omega'} \right)_{\text{incoh}}, \quad (1)$$

where  $\vec{k}_0$  and  $\vec{k}_1$  are the wave vectors of the incident and scattered neutrons, respectively,  $\vec{Q} = \vec{k}_0 - \vec{k}_1$ ,  $\hbar \omega'$  is the scattered neutron energy,  $n(\omega)$  is the Bose-Einstein factor, and  $(d^2 \sigma / d\Omega d\omega')_{\text{incoh}}$  is the double differential scattering cross section. The reconstructed  $G(\omega)$  for all scattering angles were summed up for the best averaging in the  $Q$  space. The objects used in the INS experiments were powderlike samples of deuterated lysozyme. Substitution of hydrogen by deuterium in lysozyme was achieved by dissolving it in heavy water in the presence of 0.02% sodium azide and subsequent lyophilizing.

Figure 1 shows the dependence of scattering intensity on wave vector in the double logarithmic scale for the lysozyme solution in sodium acetate buffer with a protein concentrations of 50 and 250 mg/ml obtained by SANS at 300 K. The spectrum presented in Fig. 1 is similar to those published earlier [14,15]. The  $I(q)$  dependence can be conventionally divided into three regions: the  $q < 0.1$   $\text{\AA}^{-1}$  range corresponds to the interparticle interaction between lysozyme molecules under a repulsive Coulomb potential and the 0.1–0.2 and 0.3–0.6  $\text{\AA}^{-1}$  ranges reflect mainly the tertiary protein structure and interdomain correlation within the molecule, respectively [16]. In the range of wave vectors  $0.073 < q < 0.1215$   $\text{\AA}^{-1}$  the dependence of scattering intensity on wave vector is described by the Guinier law,

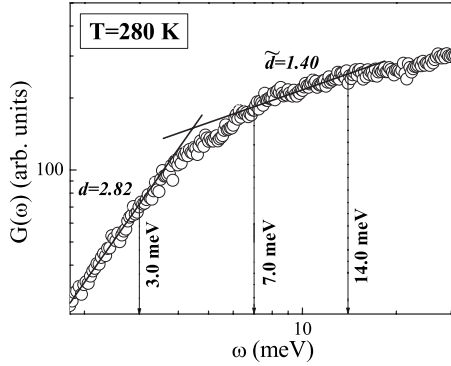


FIG. 2. Low-frequency part of the generalized density of states of lysozyme at  $T=280$  K in the log-log scale.

$$I \propto \exp(q^2 R_g^2/3), \quad (2)$$

where  $R_g$  is the gyration radius of lysozyme equal in this case to  $11.7 \pm 0.9$  Å. The gyration radius  $R_g$  obtained agrees with the literature data [14]. A small difference in the values of the radius is most likely due to a higher concentration of lysozyme in the solution used in the present study, which leads to a greater contribution of the interparticle interference effects [13]. In this paper we focus our attention on the wave-vector range  $0.1578 \text{ \AA}^{-1} < q < 0.2574 \text{ \AA}^{-1}$  that describes the spatial organization of a lysozyme molecule. The dependence of the scattering intensity on wave vector for this region is well described by the power law

$$I(q) \propto q^{-D_f}. \quad (3)$$

The linear approximation of the  $I(q)$  dependence presented in the double logarithmic interval was performed in the range  $0.1578 \text{ \AA}^{-1} < q < 0.2574 \text{ \AA}^{-1}$  by using the least-squares method. The calculations using Eq. (2) yielded  $D_f = 2.77 \pm 0.08$ . This means that lysozyme at the scales  $L < r < \xi$ , where  $L=24$  Å and correlation length  $\xi=38$  Å, can be described as a mass fractal. This range is close to the lysozyme molecule sizes, which suggests that the lysozyme molecule forms a fractal. Note that  $D_f = 2.77 \pm 0.08$  is in good agreement with the model calculations of fractal dimensions of proteins [5].

Since a lysozyme molecule is a mass fractal, its vibration spectrum must have a fracton [2]. According to the fractal approach, a fracton can be revealed by analyzing the low-frequency part of the density of states function. In the inelastic neutron scattering investigations of protonated lysozyme, a generalized density of states function  $G(\omega)$  was obtained and analyzed in the region from 1.5 to 20 meV. Note that the contribution of the multiphonon scattering is expected to be small in this region [15]. Experimental details and data processing method were described in [12]. Figure 2 shows the low-frequency region (from 1.5 to 20.0 meV) of the generalized density of states function of deuterated lysozyme  $G(\omega)$  at 280 K in the double logarithmic scale. It is well seen that the curve in Fig. 2 has two linear regions with different power law dependences. The linear approximation of these regions was performed by the least-squares method. For the  $G(\omega)$  region in the 1.5–3.5 meV energy range the exponent

has been found to be  $1.89$ , which corresponds to a spectral dimension of  $2.89 \pm 0.05$ . This result agrees with the Debye model for the density of states of acoustic modes of solids, i.e., for the energy range indicated above  $G(\omega) \propto \omega^2$ . It should be noted once more that the phonon regime was revealed earlier in studies of the low-frequency region of  $G(\omega)$  of superoxide dismutase [10]. The next linear region (Fig. 2) corresponds to the energy range from 7 to 14 meV. This region is characterized by an exponent of  $0.4$  and, hence, spectral dimension  $\tilde{d}=1.4$ . This magnitude of  $\tilde{d}$  corresponds to the fracton dimension of classical fractal systems [8]. A change in the boundaries of this region by  $\pm 1$  meV leads to a change in the spectral dimension from  $1.34$  to  $1.61$ , i.e., the error is about 10% of the initial value, which does not change the picture dramatically. Indeed, calculations have shown that the fracton dimension  $\tilde{d}$  is in the range  $1 < \tilde{d} < 2$  [8,12,17]. Comparison of  $\tilde{d}$  obtained for the deuterated and protonated [12] lysozyme has shown that they coincide within the error bars. It is important to note that there is a crossover between the two regions of the density of states function  $G(\omega)$  corresponding to the contributions of phonons and fracton. In the first approximation, we assumed that the crossover frequency  $\omega_{co}$  is the point of intersection of two straight lines obtained by the linear approximation of the regions of the density of states function of lysozyme discussed above (at  $T=280$  K,  $\omega_{co} \approx 4.5$  meV).

It should be noted that the literature data on the low-frequency dynamics of lysozyme (in the crystalline state) obtained by Raman light scattering indicate that the scattering spectra have a nonpolarized mode with frequency of  $\sim 10$  meV ( $1 \text{ meV} = 8.06 \text{ cm}^{-1}$ ) [18]. This mode is also observed in the Raman spectra of aqueous solutions of lysozyme,  $\beta$ -lactoglobulin, and other proteins [19,20]. The nature of this excitation is still unclear. Comparison of the results obtained in our studies of the vibration spectrum of lysozyme with the literature data has shown that the mode with frequency of 10 meV in the Raman spectra corresponds to the region of the generalized density of states function in the 7–14 meV energy range with spectral dimension  $\tilde{d} = 1.47$  (Fig. 2). This suggests that the mode observed by Raman scattering at the frequency of  $\sim 10$  meV is a fracton.

The fractal dimension is a measure of compactness of a protein, and therefore it must vary as the spatial structure changes. Let us see how the fractal dimension varies at thermal denaturation of lysozyme. It is evident from Fig. 1 that an increasing temperature results in a change in the slope of the curve in the range of wave vectors,  $0.1\text{--}0.2 \text{ \AA}^{-1}$ , which corresponds to a change in the fractal dimension. The temperature dependence of the fractal dimension of lysozyme obtained from the SANS data is shown in Fig. 3. It is well seen from Fig. 3 that  $D_f$  remains unaltered as temperature rises to  $\approx 333$  K. A heating from 333 to 347 K leads to a decrease in the fractal dimension (from  $2.77 \pm 0.08$  to  $2.49 \pm 0.08$ ) associated with thermal denaturation of lysozyme [21–23]. Indeed, protein disordering at denaturation results in a looser structure [14,21–23], which corresponds to a decreasing fractal dimension. At the same time, a decrease in  $D_f$  is not considerable because the spatial structure of lysozyme is stabilized by four disulfide bonds that are

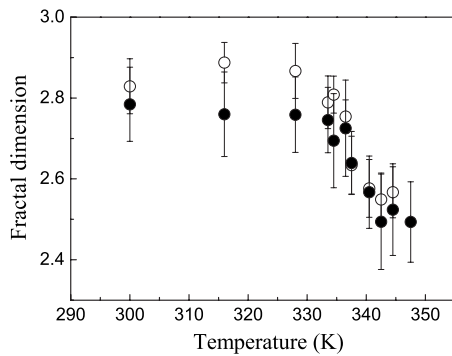


FIG. 3. Temperature dependencies of the fractal dimension of lysozyme for solutions with concentrations: 250 mg/ml (open circles); 50 mg/ml (closed circles).

not destroyed at thermal denaturation. It is important to note here some differences in the denaturation temperatures of lysozyme  $T_d$  obtained by different methods: according to calorimetric data  $T_d$  is 354 K at  $pH=4.5$  [21], while  $D_f$  reaches the minimum associated with the denaturation temperature at  $T_d \sim 342$  K. A difference of  $12^\circ$  can be attributed to the kinetics of denaturation as 342 K obtained by us is well within the width of the anomaly in the specific heat observed in Ref. [21]. Indeed, SANS measurements take a long time, which can lead to destabilization of the protein solution and, hence, a decrease in the denaturation temperature. This effect was observed earlier in IR spectroscopic studies of lysozyme [23].

An additional argument speaking in favor of the fact that it was just the lysozyme macromolecule whose changes we observed is the fact that  $D_f$  and its temperature behavior do not depend on the lysozyme concentration (see Fig. 3). It is well seen from Fig. 3 that the fractal dimensions of lysozyme in the solutions with concentrations of 50 and 250 mg/ml and their behaviors at thermal denaturation coincide within the error limits.

To summarize, the fractal dimension of lysozyme  $D_f$  has been determined and its changes at thermal denaturation have been revealed in SANS experiments. The fractal dimension of lysozyme  $\tilde{d}$  has been estimated by analyzing the generalized density of states function obtained by inelastic neutron scattering. We note here that noninteger values of the spectral dimensions  $\tilde{d}$  could be explained using various approaches (see, e.g., Refs. [24,25]). It is more difficult than, however, to explain the  $q$  dependence of the intensity in the intermediate range of wave vectors. Thus, we have succeeded in describing the lysozyme as a fractal object. This opens up possibilities for the use of the fractal approach and a corresponding mathematical technique for description of the spatial structure of proteins and their dynamics, including those at phase transformations.

The work was supported by Grants from the President of Russian Federation No. SS-2628.2008.2 and No. YK-6017.2008.2.

- 
- [1] E. Feder, *Fractals* (Plenum, New York, 1988), p. 283.
- [2] T. Nakayama, K. Yakubo, and R. L. Orbach, *Rev. Mod. Phys.* **66**, 381 (1994).
- [3] H. J. Stapleton, J. P. Allen, C. P. Flynn, D. G. Stinson, and S. R. Kurtz, *Phys. Rev. Lett.* **45**, 1456 (1980).
- [4] J. S. Helman, A. Coniglio, and C. Tsallis, *Phys. Rev. Lett.* **53**, 1195 (1984).
- [5] M. B. Enright and D. M. Leitner, *Phys. Rev. E* **71**, 011912 (2005).
- [6] S.-H. Chen and J. Teixeira, *Phys. Rev. Lett.* **57**, 2583 (1986).
- [7] D. ben-Avraham, *Phys. Rev. B* **47**, 14559 (1993).
- [8] R. Burioni *et al.*, *Proteins: Struct., Funct., and Bioinf.* **55**, 529 (2004); *Europhys. Lett.* **58**, 806 (2002); R. Granek and J. Klafter, *Phys. Rev. Lett.* **95**, 098106 (2005).
- [9] J. Smith, S. Cusack, B. Tidor, and M. Karplus, *J. Chem. Phys.* **93**, 2974 (1990).
- [10] C. Andreani, A. Deriu, A. Filabossi, and D. Russo, *Physica B* **234-236**, 223 (1997).
- [11] M. Nollmann and P. Etchegoin, *Phys. Rev. E* **60**, 4593 (1999).
- [12] S. G. Lushnikov, A. V. Svanidze, and I. L. Sashin, *JETP Lett.* **82**, 30 (2005).
- [13] D. I. Svergun and L. A. Feygin, *X-ray and Neutron Small-Angle Scattering* (Nauka, Moscow, 1986), p. 280.
- [14] H. B. Stuhmann and H. Fuess, *Acta Crystallogr., Sect. A: Cryst. Phys., Diffr., Theor. Gen. Crystallogr.* **32**, 67 (1976).
- [15] J. Smith, S. Cusack, B. Tidor, and M. Karplus, *J. Chem. Phys.* **93**, 2974 (1990).
- [16] M. Hirai, S. Arai, and H. Iwase, *J. Phys. Chem. B* **103**, 549 (1999).
- [17] M. Nollmann and P. Etchegoin, *Phys. Rev. E* **60**, 4593 (1999).
- [18] H. Urabe, Yo. Sugawara, M. Ataka, and A. Rupprecht, *Biophys. J.* **74**, 1533 (1998).
- [19] L. Genzel, F. Keilmann, T. P. Martin, G. Winterling, and Y. Yacoby, *Biopolymers* **15**, 219 (1976).
- [20] M. S. E. Colaianni and N. O. Faurskov, *J. Mol. Struct.* **347**, 267 (1995).
- [21] P. L. Privalov and N. N. Khechinashvili, *J. Mol. Biol.* **86**, 665 (1974).
- [22] D. F. Nicoli and G. B. Benedek, *Biopolymers* **15**, 2421 (1976).
- [23] R. J. Green, I. Hopkinson, and R. A. L. Jones, *Langmuir* **15**, 5102 (1999).
- [24] R. Kimmich and F. Winter, *Prog. Colloid Polym. Sci.* **71**, 66 (1985).
- [25] W. Doster, Ch. Holzhey, H. Miesmer, F. Post, and R. A. Tahir-Kheli, *J. Biol. Phys.* **17**, 281 (1990).